

---

This is an electronic reprint of the original article.  
This reprint may differ from the original in pagination and typographic detail.

Gouda, Osama E.; El Dein, Adel Z.; Tag-Eldin, Elsayed; Lehtonen, Matti; Darwish, Mohamed M.F.

## Thermal analysis of the influence of harmonics on the current capacity of medium-voltage underground power cables

*Published in:*  
Energy Science and Engineering

*DOI:*  
[10.1002/ese3.1534](https://doi.org/10.1002/ese3.1534)

Published: 01/10/2023

*Document Version*  
Publisher's PDF, also known as Version of record

*Published under the following license:*  
CC BY

*Please cite the original version:*  
Gouda, O. E., El Dein, A. Z., Tag-Eldin, E., Lehtonen, M., & Darwish, M. M. F. (2023). Thermal analysis of the influence of harmonics on the current capacity of medium-voltage underground power cables. *Energy Science and Engineering*, 11(10), 3471-3485. <https://doi.org/10.1002/ese3.1534>

## ORIGINAL ARTICLE

# Thermal analysis of the influence of harmonics on the current capacity of medium-voltage underground power cables

Osama E. Gouda<sup>1</sup> | Adel Z. El Dein<sup>2,3</sup>  | Elsayed Tag-Eldin<sup>4</sup>  |  
 Matti Lehtonen<sup>5</sup>  | Mohamed M. F. Darwish<sup>6</sup> 

<sup>1</sup>Department of Electrical Power Engineering, Faculty of Engineering, Cairo University, Giza, Egypt

<sup>2</sup>Department of Electrical Power Engineering, Faculty of Energy Engineering, Aswan University, Aswan, Egypt

<sup>3</sup>Faculty of Technological Industry and Energy, Thebes Technological University, Luxor, Egypt

<sup>4</sup>Faculty of Engineering and Technology, Future University in Egypt, New Cairo, Egypt

<sup>5</sup>Department of Electrical Engineering and Automation, Aalto University, Espoo, Finland

<sup>6</sup>Department of Electrical Engineering, Faculty of Engineering at Shoubra, Benha University, Cairo, Egypt

## Correspondence

Osama E. Gouda, Department of Electrical Power Engineering, Faculty of Engineering, Cairo University, 12613 Giza, Egypt.

Email: [prof\\_ossama11@cu.edu](mailto:prof_ossama11@cu.edu), [prof\\_ossama11@cu.edu](mailto:prof_ossama11@cu.edu) and [prof\\_ossama11@yahoo.com](mailto:prof_ossama11@yahoo.com)

Matti Lehtonen, Department of Electrical Engineering and Automation, Aalto University, 02150 Espoo, Finland.

Email: [matti.lehtonen@aalto.fi](mailto:matti.lehtonen@aalto.fi)

Mohamed M. F. Darwish, Department of Electrical Engineering, Faculty of Engineering at Shoubra, Benha University, 11629 Cairo, Egypt.

Email: [mohamed.darwish@feng.bu.edu.eg](mailto:mohamed.darwish@feng.bu.edu.eg)

## Funding information

Department of Electrical Engineering and Automation, School of Electrical Engineering, Aalto University, Espoo, Finland

## Abstract

In this article, an algorithm is proposed and used to study the influence of harmonics on the behavior of medium-voltage underground cables in flat formation. The proposed algorithm is a thermal model based on the heat equilibrium of the thermal circuit nodes of the medium-voltage cable system. The impact of harmonics on the temperature rise of the cable elements and the cable capacity is evaluated in this article. Also, the impact of harmonics on the derating factors of cable for different soil types is presented. Finally, the measurement of temperatures of cable cores is carried out experimentally and compared with the calculated results to validate the proposed algorithm. One of the algorithm merits is that several harmonic percentages can be taken into account for each cable phase individually, and the heat exchange between the cable phases and their sheath is also taken into consideration. From the obtained results, it is illustrated that the presence of harmonics has a remarkable influence on the cable core temperature; mainly, harmonics of the third and fifth orders may lead to dry zone formation around the cable. It is also observed that the presence of harmonics has an important influence on the cable current, especially when it is buried in soil that has high thermal resistivity during the summer season (suction tension =  $\infty$ ). In summer, the cable core temperature reached 152.162°C, 139.053°C, and 133.375°C when lime, sand, and silty sand, respectively, are used as backfill materials, rather than 90°C in the normal operating condition of the 11 kV three-phase

single-core cable. It is observed also that with the increase of the soil thermal resistivity, the ratio of  $(\theta_H/\theta_{\text{without harmonics}})$  reached about 1.2 times at 2.5 K m/W soil thermal resistivity. In addition, it is also observed that the impact of harmonics leads to a percentage reduction in the derating factor of the cable center phase by 11.88%–12.37% depending on the composition of the backfill materials.

#### KEYWORDS

cable capacity, derating factors, impact of harmonics, medium-voltage underground cables, thermal circuit

## 1 | INTRODUCTION

The increase in the use of power electronic devices, traction and variable speed drives, induction motors, arc welding equipment, and solid-state energy conversion devices in the industry, and domestic loads has raised the concern of the investigation of the impact of harmonics on the network components, especially the underground cables used in the distribution networks.<sup>1–3</sup> As it is known, high-, medium- (MV), and low-voltage power cables are usually used in various transmission and distribution installations. Voltage and also current harmonics delivered to the electric networks cause serious problems for these networks, such as the increase of conductors' losses, deterioration of capacitors used in improving power factor, transformers overheating, malfunction of protective relays and circuit breakers operation, and, finally, errors in electric power and energy measurement devices.<sup>4,5</sup> The additional losses, which are produced by harmonics, increase the temperatures of distribution transformers, as well as the low and medium cables of the distribution networks.<sup>6–10</sup> Some standards overlooked the influences of harmonics on the cable's current capacity assuming a balanced three-phase.<sup>11–16</sup> The accurate calculation of the cable capacity, carrying a nonsinusoidal load, is essential to re-evaluate the cable capacity to protect the cable insulation from thermal failure and for resetting the protective overcurrent relays. The neutral current of low-voltage cables, as well as the sheath current of medium cables, may be increased or greater than the phase current when the zero-sequence current, third harmonic, is presented.<sup>8</sup> This actuality causes an overheating of the neutral conductor of low-voltage cable and the metallic sheath (screen) of the MV cables unless the neutral or the sheath is properly sized. Sakis Meliopolous and colleagues<sup>17,18</sup> proposed mathematical expressions for considering the losses resulting from harmonics in the cable loading. Some authors used different algorithms to calculate the cable conductor

resistance, the cable temperature, and the cable current capacity in the presence of harmonics.<sup>17–19</sup> Practical recommendations and the requirements of the harmonic control in electrical power networks are presented in IEEE Standard 519-1992.<sup>20</sup> Hence, limits for harmonic current are tabulated in IEC1000-3-2.<sup>21</sup>

One important issue in the smart grid is to achieve the requirements of quality levels in electrical energy that match the installations of electronic switches, the new technologies of microgrids, inverters, and rectifiers,<sup>22,23</sup> which are in direct contact with the MV and low-voltage networks by using power cables. Several efforts have been made to mitigate the impact of harmonics on the electric grids.<sup>24–28</sup> Such methods are the use of reliable active harmonic filters complying with IEEE 519 and EN 50160 standards,<sup>21,29</sup> the use of rectifiers with multiple pulses, and the use of isolating transformers. Each one of the mentioned techniques has its merits and demerits, which were investigated in detail by Senthil Kumar and colleagues.<sup>24–28</sup> Gouda and colleagues<sup>30,31</sup> pointed out that the impact of harmonics has to be taken into account to accurately calculate the safe loading of underground power cables. Calculations of cable capacities, including the effects of harmonics, were carried out by Hiranandani.<sup>32</sup> Demoulias et al.<sup>33</sup> presented a method for the calculation of the capacity of low-voltage power cables under nonsinusoidal currents. A method for estimating the influence of harmonics and unbalanced currents on the capacity of concentric neutral cables was presented by Yong and Xu.<sup>34</sup> The method of calculations of low-voltage cable capacity under nonsinusoidal currents was proposed by Demoulias.<sup>35</sup>

In this paper, thermal analysis is carried out depending on the thermal equilibrium at each node of the thermal circuit of the MV cable. MV cable is defined as a cable that has a voltage rating between 1 and 30 kV. MV cables are usually solidly grounded without interchanging the cables' screens of the different phases; the cable metallic screen is directly connected to ground

potential at both ends by the use of cable terminations. Sheath bonding methods or cross-bonding grounding schemes are largely used in high-voltage cables, and they are very common for cables above 72.5 kV rating.

The impact of harmonics on the cable temperature and its current capacity are inspected with and without the existence of third, fifth, and seventh harmonics. The credibility of the proposed technique is confirmed by comparing the results obtained with the measurements done on cable feeding nonlinear loads. The impact of harmonics on the cable derating factor for different backfill soil compositions are investigated. The cable derating factor is evaluated when the cable is loaded by nonlinear loads with several harmonic orders. Finally, the proposed method investigates the influences of the cable current harmonics as well as the thermal resistivity of the backfill soils on the temperatures of the cable components.

To prove the credibility of the suggested algorithm, the cable phase's temperature is measured. It is found that the calculated temperatures by the use of the proposed method, using the finite element method (FEM), and the measured values are very close. One merit of the suggested process is that different proportions of harmonics can be considered on each phase of the cable separately, and the heat exchange between the cable phases and the cable sheath is also taken into consideration.

## 2 | THERMAL MODEL DESCRIPTION OF MV UNDERGROUND POWER CABLES

### 2.1 | Thermal model analysis

The proposed algorithm depends mainly on the thermal equilibrium at each node of the cable thermal circuit as shown in Figure 1, which simulates the medium cable system in flat formation. This model is suitable for use in the case of MV and high-voltage cables, as it takes into account the losses in the insulation material and the outer sheath, which were neglected in the low-voltage cables model.<sup>30</sup> Also, the thermal resistance of the soil between the cables in the flat formation has been taken into account<sup>30</sup>

$$W_i + \sum_{j=1}^N \left( \frac{\theta_j - \theta_i}{T_{ji}} \right) = 0. \quad (1)$$

Equation (1) represents the thermal equilibrium at each node of the cable thermal circuit as illustrated in

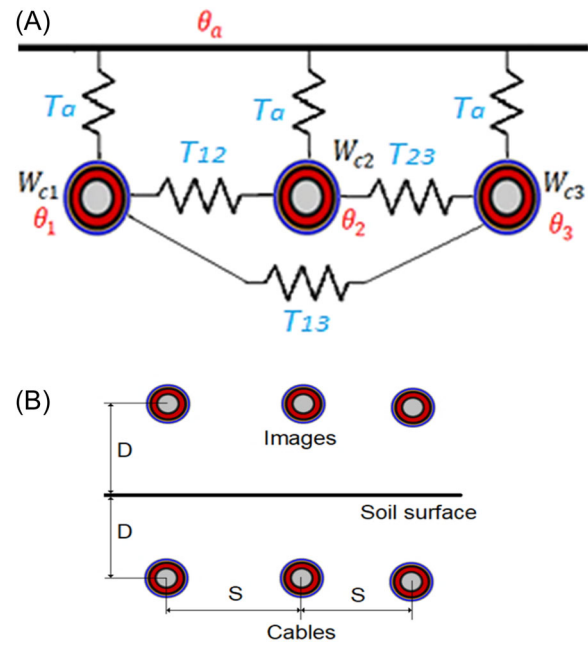


**FIGURE 1** Medium-voltage cable in flat formation: (A) the thermal circuit of the cable in flat formation and (B) its configuration.

Figure 1, where  $W_i$  is defined as the summation of cable losses at node  $i$ ,  $\theta_j - \theta_i$  is the temperature difference between every two nodes, and  $T_{ji}$  is the thermal resistance between every two nodes. Referring to Figure 1, there are three thermal paths for heat loss in each phase of the cable. In phase A, the first path is through thermal resistance ( $T_{11}$ ) in the direction of the air temperature, the second is in the direction of phase B through thermal resistance ( $T_{12}$ ), and the third is in the direction of phase C through the thermal resistance ( $T_{13}$ ). Similar paths are shown in Figure 1 for phases B and C.  $T_{1a}$ ,  $T_{2a}$ , and  $T_{3a}$  are the thermal resistances between phases A, B, and C and ambient (they are equal and shown in Figure 1 as  $T_a$ ). Applying Equation (1) to the case under study, at the  $h$ th harmonic, gives a set of equations, which relate the temperatures, thermal resistances, and heat sources, as well as the thermal coupling, between the three phases of the underground MV cable, as illustrated in Equation (2)

$$\begin{bmatrix} \frac{1}{T_{11}} & \frac{-1}{T_{12}} & \frac{-1}{T_{13}} \\ \frac{-1}{T_{21}} & \frac{1}{T_{22}} & \frac{-1}{T_{23}} \\ \frac{-1}{T_{31}} & \frac{-1}{T_{32}} & \frac{1}{T_{33}} \end{bmatrix} \begin{bmatrix} \theta_1(h) \\ \theta_2(h) \\ \theta_3(h) \end{bmatrix} = \begin{bmatrix} W_{c1}(h) + W_{d1}(h)F + \frac{\theta_a}{T_{1a}} \\ W_{c2}(h) + W_{d2}(h)F + \frac{\theta_a}{T_{2a}} \\ W_{c3}(h) + W_{d3}(h)F + \frac{\theta_a}{T_{3a}} \end{bmatrix}. \quad (2)$$

The losses  $W_{c1}(h)$ ,  $W_{c2}(h)$ , and  $W_{c3}(h)$  are the copper losses of each phase in the presence of harmonics.  $W_{d1}(h)$ ,  $W_{d2}(h)$ , and  $W_{d3}(h)$  are the dielectric losses of

each phase in the presence of harmonics.  $F$  is a factor that has been defined in Equation (11). Hence, an increase in the cable core temperatures in the three phases due to  $h$ th harmonics can be obtained by using Equation (3)

$$\begin{bmatrix} \Delta\theta_1(h) \\ \Delta\theta_2(h) \\ \Delta\theta_3(h) \end{bmatrix} = \begin{bmatrix} \frac{1}{T_{11}} & \frac{-1}{T_{12}} & \frac{-1}{T_{13}} \\ \frac{-1}{T_{21}} & \frac{1}{T_{22}} & \frac{-1}{T_{23}} \\ \frac{-1}{T_{31}} & \frac{-1}{T_{32}} & \frac{1}{T_{33}} \end{bmatrix}^{-1} \begin{bmatrix} W_{c1}(h) + W_{d1}(h)F + \frac{\theta_a}{T_{1a}} \\ W_{c2}(h) + W_{d2}(h)F + \frac{\theta_a}{T_{2a}} \\ W_{c3}(h) + W_{d3}(h)F + \frac{\theta_a}{T_{3a}} \end{bmatrix} - \theta_a. \quad (3)$$

Then, the cable core temperatures of the three phases with harmonics can be obtained using Equation (4)

$$\begin{bmatrix} \theta_{t1} \\ \theta_{t2} \\ \theta_{t3} \end{bmatrix} = \theta_a + \begin{bmatrix} \sum_{h=1}^{\infty} \Delta\theta_1(h) \\ \sum_{h=1}^{\infty} \Delta\theta_2(h) \\ \sum_{h=1}^{\infty} \Delta\theta_3(h) \end{bmatrix}. \quad (4)$$

It is important to obtain the cable core temperatures by using Equation (4);  $T_{ii}$  is the self-thermal resistance of the cable  $i$ , and it is obtained by using Equation (5)

$$\frac{1}{T_{ii}} = \frac{1}{T_{ia}} + \sum_{n=1}^m \frac{1}{T_{in}}, \quad (5)$$

where

$$T = \frac{T_1}{n} + (1 + \lambda_1)T_2 + (1 + \lambda_1 + \lambda_2)T_3,$$

$$T_{1a} = T + T_4(1 + \lambda_1 + \lambda_2) = T_{2a} = T_{3a} = T_a,$$

$T_{12} = T_{21}$ ,  $T_{13} = T_{31}$ , and  $T_{23} = T_{32}$  are the thermal resistances between phases A, B, and C as shown in Figure 1.

$$\frac{1}{T_{11}} = \frac{1}{T_{12}} + \frac{1}{T_{13}} + \frac{1}{T_{1a}}, \frac{1}{T_{22}} = \frac{1}{T_{21}} + \frac{1}{T_{23}} + \frac{1}{T_{2a}}, \text{ and } \frac{1}{T_{33}} = \frac{1}{T_{31}} + \frac{1}{T_{32}} + \frac{1}{T_{3a}},$$

$$T_d = \frac{T_1}{2n} + T_2 + T_3,$$

where  $T_1$ ,  $T_2$ ,  $T_3$ , and  $T_4$  are the thermal resistances of cable dielectric, cable sheath, cable jacket, and backfill soil, respectively,  $n$  is defined as the cable conductors

number,  $\lambda_1$  and  $\lambda_2$  are the ratios between the metal sheath and armoring losses from one side and total losses in that cable on the other side, respectively. The sheath temperature at any harmonic order  $h$  can be calculated by using equations:

$$\theta_{sh1} = \theta_{c1} - (W_{c1}(h) + W_{d1}(h)/2)T_d, \quad (6)$$

$$\theta_{sh2} = \theta_{c2} - (W_{c2}(h) + W_{d2}(h)/2)T_d, \quad (7)$$

$$\theta_{sh3} = \theta_{c3} - (W_{c3}(h) + W_{d3}(h)/2)T_d. \quad (8)$$

The proposed thermal model can be generalized to any cable arrangement, such as trefoil formation, taking into account changing the values of thermal resistances  $T_{12}$ ,  $T_{13}$ , and  $T_{23}$ .

## 2.2 | Impact of harmonics on the cables' derating factors

Once the cable core temperatures of the three phases are calculated using Equation (4), they should be checked; if they exceed the permissible maximum operating temperature (90°C), new cable capacities can be obtained and compared with the previous load currents. The capacities of the cable's three phases, with the harmonic occurrence, can be obtained by using Equation (9)

$$\begin{bmatrix} I_1 \\ I_2 \\ I_3 \end{bmatrix} = \begin{bmatrix} \frac{1}{\beta_1} \left\{ \frac{\theta_{c1}}{T_{11}} - \frac{\theta_{c2}}{T_{12}} - \frac{\theta_{c3}}{T_{13}} - \frac{\theta_a}{T_{1a}} - W_{d1}(h)F \right\} \\ \frac{1}{\beta_2} \left\{ -\frac{\theta_{c1}}{T_{12}} + \frac{\theta_{c2}}{T_{22}} - \frac{\theta_{c3}}{T_{23}} - \frac{\theta_a}{T_{2a}} - W_{d2}(h)F \right\} \\ \frac{1}{\beta_3} \left\{ -\frac{\theta_{c1}}{T_{31}} - \frac{\theta_{c2}}{T_{32}} + \frac{\theta_{c3}}{T_{33}} - \frac{\theta_a}{T_{3a}} - W_{d3}(h)F \right\} \end{bmatrix}, \quad (9)$$

where  $\theta_{c1}$ ,  $\theta_{c2}$ , and  $\theta_{c3}$  are the operating temperatures of cable conductors and  $\beta_i$  is defined as given in Equation (10), as the inverse of the sum of AC resistance at the harmonic order ( $h$ ) multiplied by the square of the modulus  $\alpha_i(h)$

$$\beta_i = \frac{1}{\sum_{h=1}^{\infty} r_{ac}(h)\alpha_i^2(h)}, \quad (10)$$

$$F = \frac{2T + (1 + \lambda_1 + \lambda_2)(T_d + 3T_4)}{(1 + \lambda_1 + \lambda_2)(T + T_4(1 + \lambda_1 + \lambda_2))}, \quad (11)$$

where  $\alpha_i(h)$  is defined as given in Equation (12)

$$\alpha_i(h) = \frac{I_i(h)}{I_{i,\text{fund}}}, \quad (12)$$

where  $I_i(h)$  is the  $h$ th harmonics current of cable  $i$ th, and  $I_{i,\text{fund}}$  is the fundamental current of cable  $i$ th.

The re-evaluation coefficient (derating factor) can be defined as the ratio between the values of the cable current in the presence of harmonics at the actual temperature  $\theta$ , which can be obtained using Equation (9), and the cable current when the conductor temperature reaches 90°C.

The derating factor considering the impact of harmonics  $D_H$  can be obtained by using Equation (13)

$$D_H = \frac{I(\theta)}{I(90)}, \quad (13)$$

### 2.3 | Thermal resistances of the cable components and backfill soils

According to IEC60287,<sup>11</sup> the thermal resistances of the cable components and the cable backfill soil can be obtained using Equations (14)–(17), respectively,

$$T_1 = \frac{\rho_d}{2\pi} \ln\left(\frac{r_d}{r_c}\right) \text{ is dielectric thermal resistance,} \quad (14)$$

$$T_2 = \frac{\rho_{sh}}{2\pi} \ln\left(\frac{r_{sh}}{r_d}\right) \text{ is the sheath thermal resistance,} \quad (15)$$

$$T_3 = \frac{\rho_j}{2\pi} \ln\left(\frac{r_j}{r_{sh}}\right) \text{ is the jacket's thermal resistance,} \quad (16)$$

$$T_4 = \frac{\rho_{soil}}{2\pi} \ln\left(\frac{4D}{D_c}\right) \text{ is the external thermal resistance.} \quad (17)$$

The thermal resistance between two phases, as shown in Figure 1B, can be obtained using Equation (18)

$$T_{ij} = \frac{\rho_{soil}}{2\pi} \ln\left(\frac{D_{ij}}{d_{ij}}\right), \quad (18)$$

where  $\rho_d$  is the thermal resistivity of cable dielectric,  $\rho_{sh}$  is the sheath thermal resistivity,  $\rho_j$  is the jacket thermal resistivity,  $\rho_{soil}$  the soil thermal resistivity,  $r_c$  the conductor radius,  $r_d$  the insulation outer radius,  $r_{sh}$  the sheath outer radius,  $r_j$  the jacket outer radius,  $D$  the cable laying depth,  $d_c$  the conductor diameter,  $D_c$  the cable outer diameter,  $D_{ij}$  the distance between the  $i$ th cable center and the center of the image of  $j$ th cable,  $d_{ij}$  the distance between the  $i$ th cable center and the center of  $j$ th cable,

and  $T_{ii}$  the self-thermal resistance of the  $i$ th cable, and it is defined as given in the following relation:

$$\frac{1}{T_{ii}} = \frac{1}{T_{ia}} + \sum_{\substack{n=1 \\ n \neq i}}^m \frac{1}{T_{in}}.$$

### 2.4 | Impact of harmonics on cable losses

The total conductor loss of each phase at any harmonic order can be obtained by using Equations (19) or (20):

$$Wc(h) = I(h)^2 r_{ac}(h), \quad (19)$$

$$Wc(h) = \alpha_i^2(h) I_{i,\text{fund}}^2 r_{ac}(h), \quad (20)$$

where  $I(h)$  is the cable current component that contains  $h$ th harmonic order,  $I_{i,\text{fund}}$  is the fundamental current of the cable in RMS, and  $r_{ac}(h)$  is the AC resistance of cable conductor at the  $h$ th harmonic in ( $\Omega/\text{m}$ ). It can be obtained by Equation (21)

$$r_{ac}(h) = r_{dc}(1 + Y_s(h) + Y_p(h))[1 + a_{20}(\theta - 20)], \quad (21)$$

where  $r_{dc}$  is the DC resistance of the cable conductor at the ambient temperature in ohms per meter,  $Y_p(h)$  is the proximity effect factor,  $\lambda_1(h)$  is the sheath loss factor,  $Y_s(h)$  is the skin effect factor, which, in IEC60287-1-2,<sup>11</sup> is defined as

$$Y_s(h) = \frac{x_s^4}{192 + 0.8x_s^4},$$

$$x_s^4(h) = \frac{8\pi f(h)k_s 10^{-7}}{r_{dc}},$$

where  $k_s$  is the coefficient factor of the skin effect and  $f(h)$  is the harmonic frequency at order  $h$ .  $Y_p(h)$  is the proximity factor, which is defined by IEC60287-1-2<sup>11</sup>

$$Y_p(h) = \frac{x_p^4}{192 + 0.8x_p^4} \left(\frac{d_c}{S}\right)^2 \left[ 0.312 \left(\frac{d_c}{S}\right)^2 + \frac{1.18}{\frac{x_p^4}{192 + 0.8x_p^4} + 0.27} \right],$$

$$x_p^4(h) = \frac{8\pi f(h)k_p 10^{-7}}{R_{dc}},$$



in which  $S$  is the space in meters between cables' core axes,  $k_p$  is the coefficient factor of the proximity effect,  $\alpha_{20}$  is the coefficient of conductor temperature,  $\theta$  the conductor temperature. The dielectric loss at each harmonic order is calculated as follows:

$$Wd(h) = 2\pi f(h)CV_0^2 \tan \delta, \quad (22)$$

where  $f(h)$  means the harmonic order frequency,  $V_0$  depicts the rated voltage per phase, and  $C$  represents the electrical capacitance, which is obtained as follows:

$$C = \frac{\varepsilon}{18 \ln \left( \frac{D_i}{d_c} \right)}, \quad (23)$$

where  $\varepsilon$  is the insulator's relative permittivity,  $D_i$  means the outer diameter of the insulator, and  $d_c$  indicates the conductor diameter in meters. For the calculations of sheath and armor losses,  $\lambda_1(h)$  and  $\lambda_2(h)$  are considered as the sheath and armor loss factors that are generated by each harmonic order of each cable phase, respectively, according to IEC60287.

### 3 | CABLE DATA, HARMONICS, AND CORE TEMPERATURE MEASUREMENTS

Because the proposed algorithm can be used to study the impact of harmonics on all medium- and high-voltage cables, the dielectric, sheath, and armor losses are considered in the case under the study of 11 kV feeders, although they can be ignored.

#### 3.1 | Data of the cable under study

The flat configuration of the 11 kV cables, which is usually used in the distribution system, is considered as a case study in this article. It has consisted of three single cores. The CYMCAP software (<https://www.cyme.com/software/cymcap/>) is used in the simulation of the cable under study according to International Standards IEC60287.<sup>11</sup>

Figure 2 shows the construction of the 11 kV single-core cable; its conductor diameter equals 40.2 mm, insulation outer diameter is 54.3 mm, sheath outer diameter equals 58.8 mm, and jacket outer diameter is 65.4 mm. The cable-rated current is 2.04 kA per phase at a laying depth equal to 1 m. The backfill material is sandy soil. The thermal resistivity of this soil type is 1.2 K m/W at 35°C air temperature. The core cable operating temperature is

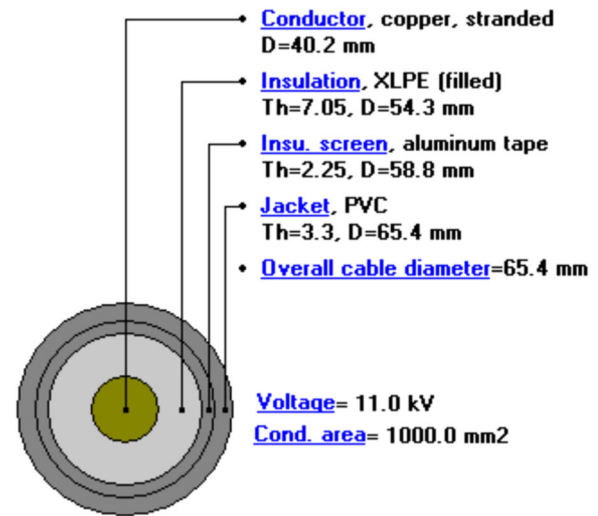


**FIGURE 2** Construction of the 11 kV single-core cable. PVC polyvinyl chloride; XLPE, cross-linked polyethylene.

90°C, and its insulation is cross-linked polyethylene with polyvinyl chloride cable jacketing. The cable is earthed from both ends, and no armoring layer is used.

#### 3.2 | Harmonic measurements

Generally, investigating harmonic conditioning of the lowest orders is appropriate. Utilities and industrial loads are mainly focusing on harmonics of low orders like third, fifth, seventh, 11th, and 13th. As it is known, harmonic analyzers are used in the measurement, management, monitoring, and analysis of the parameters of electrical grids such as current, power factor, voltage, harmonic distortion, and power quality. Most of the harmonics analyzers are used in measuring the electrical parameters of three-phase and four-wire asymmetrical and symmetrical grids and for monitoring the total harmonic distortion (THD) factor.

In this study, PQ3350 three-phase power and harmonics analyzer is used in the measurement of harmonics of the 11 kV feeder of an industrial load of Mass food factory at Six October industrial zone, Egypt. The analyzer complies with IEC61000-4-7 standard.<sup>36</sup> The PQ3350 analyzer has the ability to measure and analyze voltage and current harmonic distortion, the current and voltage harmonic spectrum,  $K$  factor for harmonics, and the phase angle between harmonic voltage and current, up to the 39th order. The sampling rate of PQ3350 is 128 samples for each cycle. The harmonic measurements of industrial feeders are carried out according to IEC61000-3-2.<sup>21</sup> The average of the measured values of the third, fifth, seventh, 11th, and 13th harmonic orders of phases A, B, and C are illustrated in

**TABLE 1** Harmonic measurements in the tested feeder.

| Cable phase  | Fundamental current (%) | Average third harmonic (%) | Average fifth harmonic | Average seventh harmonic (%) | Average 11th harmonic (%) | Average 13th harmonic (%) | Average THD (%) |
|--------------|-------------------------|----------------------------|------------------------|------------------------------|---------------------------|---------------------------|-----------------|
| A            | 100                     | 31.5                       | 29.5                   | 6.45                         | 0.37                      | 0.25                      | 43.65           |
| B            | 96                      | 28                         | 28.7                   | 6.7                          | 0.51                      | 0.43                      | 40.66           |
| C            | 97                      | 32                         | 25.29                  | 8.5                          | 0.21                      | 0.15                      | 41.67           |
| Cable screen | 7                       | 91.5                       | 0                      | 0                            | 0                         | 0                         | —               |

Abbreviation: THD, total harmonic distortion.

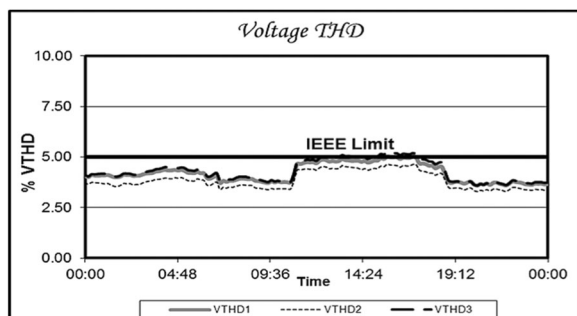
**FIGURE 3** Voltage harmonic (total harmonic distortion [THD]) as a function of time.

Table 1. In the cable screen, the third harmonic has existed as given in Table 1. From the measurements done, it is observed that the voltage THD values are within the IEEE limit or even less, as given in Figure 3. The current harmonic distortion (THD) versus time is given in Figure 4, and its average value for each phase is shown in Table 1. As it is noticed, current THD values exceed the IEEE limit. Note that the reason for the absence of the fifth, seventh, 11th, and 13th harmonics on cable sheaths (see Table 1) is due to the currents of these frequencies on the three-phase conductors being balanced. Thus, these currents on the three sheaths cancel out each other at each frequency and cannot be captured in the field measurement. In contrast, the third harmonic-induced currents on the three sheaths add up due to their zero-sequence nature.

### 3.3 | Measurement of cable core temperatures

Thermocouple groups are used for measuring the conductor temperature of each cable phase. The thermocouples are located along the tested length of the cable (10 m for each phase). The distance between each of the two adjacent thermocouples was about a meter. Table 2 illustrates the average values of each cable phase temperature when the cable is loaded by the rated

current at 35°C air temperature and 1-m laying depth. The soil thermal resistivity was 1.2°C m/W.

## 4 | RESULTS AND DISCUSSION

### 4.1 | Impact of harmonics on the three-phase cable core temperatures using the thermal model

By using the proposed thermal model, Table 2 clarifies the impact of harmonic orders on the cable phases temperatures, where  $\Delta\theta_{\text{without har}}$ ,  $\Delta\theta_1$ ,  $\Delta\theta_3$ ,  $\Delta\theta_5$ ,  $\Delta\theta_7$ , and  $\Delta\theta_H$  are the difference between the core cable temperature and air temperature neglecting the influence of harmonics and after adding the third, fifth, and seventh harmonics to the 50 Hz current. The calculations are done at an air temperature of 35°C, the thermal resistivity of backfill soil was 1.2 K m/W, and when the cable is loaded by 2040 A and buried at a laying depth of 1 m. It is noticed that the harmonic temperature  $\theta_H$  surpassed the allowable cable temperature (90°C) by about 14.1°C for phases A and C and 16.2°C for phase B, while the sheath temperature reached 82.585°C for phases A and C and 87.633°C for phase B. From Table 2, it is noticed that the temperature measurements and the calculations done by using the proposed algorithm are in agreement. When the cable conductor temperature exceeds its permissible operating temperature (above 90°C), it is necessary to either reduce the cable load or use filters to eliminate harmful harmonics or replace some of the nonlinear loads of the feeder.

### 4.2 | Soil decomposition influence on the temperature of the cable core in the presence of harmonics

The aim of this section is to study the effect of harmonics in the case of burying medium-voltage cables in different types of soils, especially cables installed in flat formations



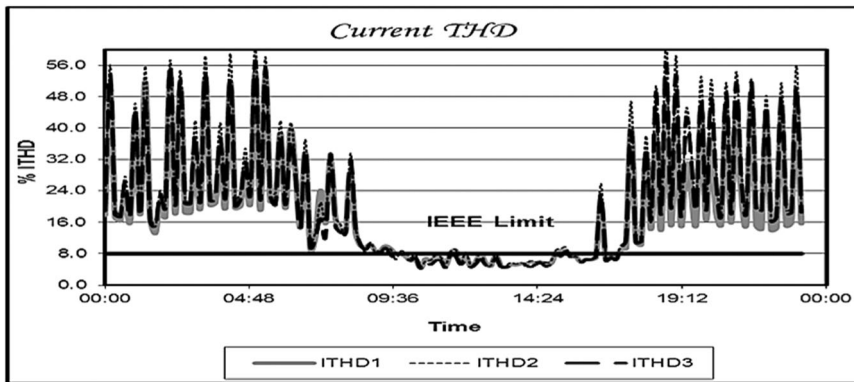


**FIGURE 4** Current harmonic distortion (total harmonic distortion [THD]) as a function of time.

**TABLE 2** Impact of harmonics on cable core temperatures.

|                             | $\Delta\theta_{\text{without harmonics}}$<br>or $\Delta\theta_1$ (°C) | $\Delta\theta_3$ (°C) | $\Delta\theta_5$ (°C) | $\Delta\theta_7$ (°C) | $\Delta\theta_H$ (°C) | $\theta_H$ (°C)<br>Calculated | $\theta_H$ (°C)<br>Measured |
|-----------------------------|---|-----------------------|-----------------------|-----------------------|-----------------------|-------------------------------|-----------------------------|
| Cable phase                 |   |                       |                       |                       |                       |                               |                             |
| A                           | 55.569  | 6.458                 | 6.804                 | 0.319                 | 69.151                | 104.151                       | 105.5                       |
| B                           | 56.974  | 6.664                 | 6.918                 | 0.52                  | 71.076                | 106.076                       | 107                         |
| C                           | 55.569  | 6.458                 | 6.804                 | 0.319                 | 69.151                | 104.151                       | 105.9                       |
| Screen (sheath) temperature |   |                       |                       |                       |                       |                               |                             |
| A                           | 37.749  | 4.571                 | 5.043                 | 0.222                 | 47.585                | 82.585                        | 83.5                        |
| B                           | 41.475  | 5.312                 | 5.42                  | 0.426                 | 52.633                | 87.633                        | 88                          |
| C                           | 37.749  | 4.571                 | 5.043                 | 0.222                 | 47.585                | 82.585                        | 83.7                        |

in which the soil plays an important role in the dissipation of heat resulting from harmonics; this issue was not previously studied. Table 3 illustrates the influence of different soil components on the (phase B) temperature when harmonics influences are considered. Phase B is selected because it is the hottest one of the cable phases as it is illustrated in Table 2. The specifications of the backfill soil are measured by using a similar technique that is proposed by Gouda et al.<sup>37–39</sup> The experimental data are originally presented in Gouda et al.<sup>38</sup> In Table 3,  $\rho_{\text{dry}}$  is the dry thermal soil resistivity,  $\rho_{\text{wet}}$  is the wet thermal resistivity of the soil,  $\theta_x$  is the critical soil temperature, and  $pf$  is the soil suction tension; it is defined as:  $pf = \log(-100\varphi)$  (24), where ( $\varphi$ ) means the moisture potential.

According to the proposed technique by Gouda et al.,<sup>37–39</sup> the tests were conducted to measure the thermal resistance of each soil separately while the soil suction tension was changed to be 1, 2, and  $\infty$  sequentially by changing the water column of the device used in the laboratory. The measured values are illustrated in Table 3. The importance of using the suction tension in this article as a variable factor is that it illustrates the impact of the water table level influence on

the soil in different yearly seasons. Usually, the suction tension in winter can be taken as 1, while it can be considered as  $\infty$  in summer.

In other seasons, the suction tension value is taken 2. As shown in Table 3, the cable core temperature has a significant increase in summer ( $pf = \infty$ ) compared with other seasons ( $pf = 1$  in winter and 2 in other seasons).

From Table 3, it is noticed that the presence of harmonics increases the cable core temperature, regarding the surrounding soil composition. The combination of the presence of harmonics in the cable core and the formation of a dry zone around the cable increases the cable core temperature to severe values. In summer ( $pf = \infty$ ), it reached 152.162°C, 139.053°C, and 133.375°C when lime, sand, and silt + sand are used as backfill materials, respectively.

In general, the impact of the soil thermal resistivity on the cable operating temperature can be illustrated as given in Figure 5. This figure shows the relation between the ratio of the cable core temperature with harmonic impact and ignoring the influence of harmonics ( $\theta_H / \theta_{\text{without harmonics}}$ ). As it is observed, with the increase of the soil thermal resistivity, the ratio of ( $\theta_H / \theta_{\text{without harmonics}}$ ) reaches about 1.2 when soil thermal resistivity equals 2.5 K m/W.

**TABLE 3** Temperature of phase B conductor loaded by its rated current for different backfill soils without and with the impact of harmonics, 11 kV cable rating.

| Soil type           | $\rho_{\text{dry}}$<br>(°C m/w) | $\rho_{\text{wet}}$<br>(°C m/w) | $\theta_x$ | $pf$     | Cable core temperature at 2040 A (°C)<br>11 kV |               |                    |               |
|---------------------|---------------------------------|---------------------------------|------------|----------|--|---------------|--------------------|---------------|
|                     |                                 |                                 |            |          | With harmonics                                 |               | Ignoring harmonics |               |
|                     |                                 |                                 |            |          | Without dry Zone                               | With dry Zone | Without dry Zone   | With dry Zone |
| Lime                | 2.35                            | 0.941                           | 62         | $\infty$ | 93.338   | 152.162       | 81.885             | 129.128       |
|                     | 1.8                             | 0.85                            | 56         | 2        | 89.539   | 129.2         | 78.833             | 110.687       |
|                     | 1.7                             | 0.76                            | 58         | 1        | 85.781   | 125.025       | 75.816             | 107.334       |
| 25% Lime + 75% sand | 1.304                           | 0.522                           | 62         | $\infty$ | 75.845   | 108.493       | 67.835             | 94.056        |
|                     | 1.22                            | 0.50                            | 60         | 2        | 74.926   | 104.986       | 67.098             | 91.239        |
|                     | 1.02                            | 0.48                            | 58         | 1        | 74.091   | 96.636        | 66.427             | 84.533        |
| Clay                | 1.586                           | 0.627                           | 60         | $\infty$ | 80.228   | 120.266       | 71.356             | 103.511       |
|                     | 1.53                            | 0.61                            | 58         | 2        | 79.519   | 117.928       | 70.786             | 101.634       |
|                     | 1.51                            | 0.60                            | 58         | 1        | 78.321   | 117.093       | 70.212             | 100.963       |
| Sand                | 2.036                           | 0.968                           | 62         | $\infty$ | 94.465   | 139.053       | 82.79              | 118.6         |
|                     | 1.7                             | 0.75                            | 56         | 2        | 85.364   | 125.025       | 75.48              | 107.334       |
|                     | 1.46                            | 0.73                            | 58         | 1        | 84.132   | 115.005       | 74.721             | 99.287        |
| Clay + silt + sand  | 1.69                            | 0.83                            | 60         | $\infty$ | 88.704   | 124.608       | 78.163             | 106.998       |
|                     | 1.6                             | 0.756                           | 58         | 2        | 85.614   | 120.85        | 75.682             | 103.981       |
|                     | 1.469                           | 0.705                           | 64         | 1        | 83.485   | 115.381       | 73.971             | 99.588        |
| Silt + sand         | 1.9                             | 0.756                           | 56         | $\infty$ | 85.614   | 133.375       | 75.682             | 114.04        |
|                     | 1.68                            | 0.66                            | 54         | 2        | 81.606   | 124.19        | 72.463             | 106.663       |
|                     | 1.5                             | 0.67                            | 60         | 1        | 82.024   | 116.675       | 72.798             | 100.628       |

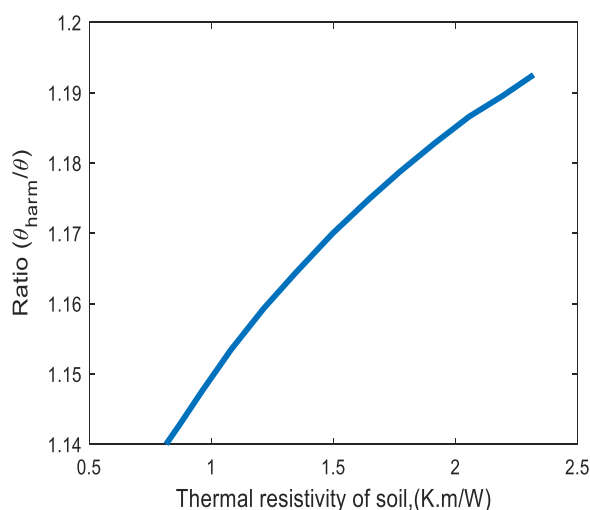


**FIGURE 5**  $(\theta_H/\theta_{\text{without harmonics}})$  as a function of the thermal resistivity of the backfill soil.

### 4.3 | Impact of harmonics on the cable derating factor

Table 4 illustrates the impact of harmonics on the current capacity of phase B (center phase) at different backfill soil compositions and different yearly seasons (change in suction tension). The calculations are done by using the proposed thermal model.

It is clear that the combination of the presence of harmonics in the cable core and the formation of a dry zone around the cable reduces the cable current capacity regardless of the soil components surrounding the cable. By dividing the current of the center cable core with harmonics in cases of wet and dry soils by the value of core-rated current at temperature 90°C, the derating factors can be calculated as follows:

**TABLE 4** Influence of harmonics on the center phase of cable current capacities at different backfill soil compositions at 35°C ambient temperature, 11 kV cable rating.

| Soil type           | Current capacity of the cable in (kA) |               |                   |               |
|---------------------|---------------------------------------|---------------|-------------------|---------------|
|                     | With harmonics                        |               | Without harmonics |               |
|                     | Without dry zone                      | With dry zone | Without dry zone  | With dry zone |
| Lime                | 1.984                                 | 1.4           | 2.221             | 1.567         |
|                     | 2.052                                 | 1.561         | 2.297             | 1.748         |
|                     | 2.126                                 | 1.597         | 2.38              | 1.788         |
| 25% Lime + 75% sand | 2.371                                 | 1.768         | 2.654             | 1.979         |
|                     | 2.398                                 | 1.811         | 2.684             | 2.028         |
|                     | 2.423                                 | 1.93          | 2.712             | 2.161         |
| Clay                | 2.253                                 | 1.641         | 2.522             | 1.837         |
|                     | 2.271                                 | 1.664         | 2.542             | 1.863         |
|                     | 2.271                                 | 1.673         | 2.542             | 1.872         |
| Sand                | 1.965                                 | 1.486         | 2.2               | 1.663         |
|                     | 2.135                                 | 1.597         | 2.39              | 1.788         |
|                     | 2.135                                 | 1.694         | 2.39              | 1.897         |
| Clay + silt + sand  | 2.068                                 | 1.601         | 2.315             | 1.792         |
|                     | 2.13                                  | 1.636         | 2.384             | 1.831         |
|                     | 2.176                                 | 1.69          | 2.436             | 1.892         |
| Silt + sand         | 2.13                                  | 1.528         | 2.384             | 1.71          |
|                     | 2.219                                 | 1.605         | 2.484             | 1.796         |
|                     | 2.21                                  | 1.677         | 2.473             | 1.877         |

$$D_{\text{with harmonics}} = \frac{I(\text{with harmonics})}{I(90)}, \quad (24)$$

in which  $D_{\text{with harmonics}}$  represents the derating factor caused by the impact of harmonics

$$D_{\text{without harmonics}} = \frac{I(\text{without harmonics})}{I(90)}, \quad (25)$$

where  $D_{\text{without harmonics}}$  means the derating factor ignoring the impact of harmonics.

The calculations of the derating factors of the cable center phase with and without the presence of harmonics are presented in Table 5. From this table, it is observed that the occurrence of harmonics has a respectable impact on the cable current, especially when it is buried in soil with high thermal resistivity during the summer season ( $pf = \infty$ ).

In Table 5, the impact of harmonics on the cable derating factor is calculated using Equation (26)

$$\% \text{ Change in derating factor due to the impact of harmonics} = \frac{I(\text{without harmonics}) - I(\text{with harmonics})}{I(\text{without harmonics})}. \quad (26)$$

It is noticed in Table 5 that the percentage reduction in the derating factor of the center phase (B) caused by the impact of harmonics differs between 11.88% and 12.37% depending on the soil composition that is surrounding the cable. In general, the ratio between the current of the center cable core at the permissible maximum operating temperature (90°C) and the current calculated in the presence of harmonics at different soil resistivities is given in Figure 6 at an ambient temperature equal to 35°C. Figure 7 clarifies the impact of the cable laying depth on the ratio between the cable conductor temperature in the presence of harmonics and the maximum permissible conductor temperature of the cable for the 11 kV cable. According to IEC60287, the laying depth of medium-voltage cables is between 0.8 and 1.5 m. Table 6 illustrates the impact of the cable laying depth on the conductor temperature in the presence of harmonics. From Table 6, it is clear that with the increase of the cable laying depth from 0.5 to 1.5 m, the temperature of the cable conductor increases from 94°C to 110°C.

#### 4.4 | Effect of axial spacing between cable phases on the cable core temperature

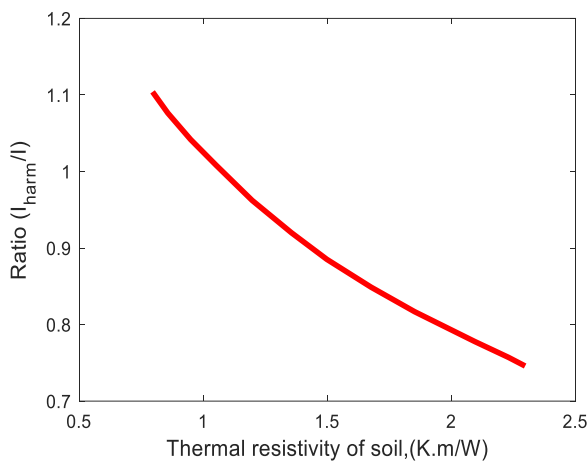
Table 7 illustrates the effect of the axial spacing between cable phases on each phase temperature when the harmonics are taken into consideration. It is clear that the axial spacing between the cable phases has a slight effect on its operating temperature; when the axial spacing between cables increases from 127 to 200 mm, the operating temperature decreases from 106.076°C to 105.867°C. From Figure 7, it is observed that with the increase of air temperature ( $\theta_a$ ) from 30°C to 45°C, the ratio between the conductor temperatures in the presence and/or absence of harmonics ( $\theta_H/\theta_{\text{without har}}$ ) is increased.

### 5 | MAP OF THE CABLE ELEMENTS AND ITS BACKFILL SOIL TEMPERATURES USING COMSOL MULTIPHYSICS PROGRAM AND FEM

As it is known, the cable length is usually larger than its laying depth, so the issue becomes a two-dimensional heat conduction problem. To solve the problems of

**TABLE 5** Summary of derating factors of the center phase with harmonics and without harmonics at 35°C ambient temperature.

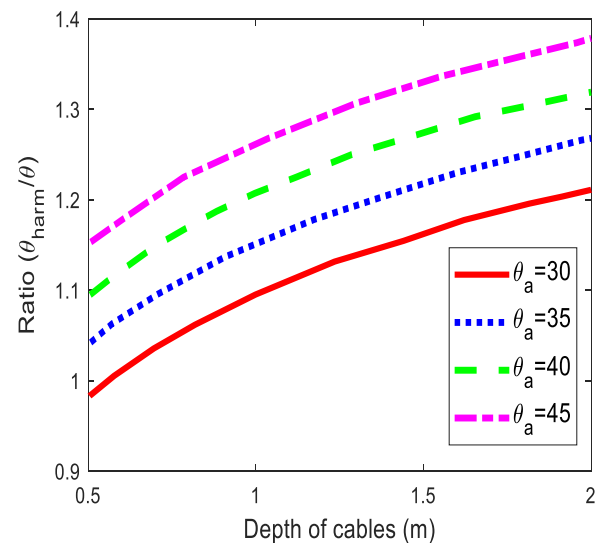
| Soilmaterial        | $pf$ suction tension | $D_{HW}$ of the center phase with harmonics | $D_{HD}$ of the center phase without harmonics | % Change in derating factor due to the impact of harmonics |
|---------------------|----------------------|---|--|--|
| Lime                | $\infty$             | 0.686                                       | 0.768  | 11.9   |
|                     | 2                    | 0.765                                       | 0.856  | 11.89  |
|                     | 1                    | 0.782                                       | 0.876  | 12.02  |
| 25% Lime + 75% sand | $\infty$             | 0.866                                       | 0.970  | 12.009   |
|                     | 2                    | 0.887                                       | 0.994  | 12.06  |
|                     | 1                    | 0.946                                       | 1.059  | 11.94  |
| Clay                | $\infty$             | 0.804                                       | 0.900  | 11.94  |
|                     | 2                    | 0.816                                       | 0.913  | 11.88  |
|                     | 1                    | 0.816                                       | 0.917  | 12.37  |
| Sand                | $\infty$             | 0.728                                       | 0.815  | 11.95  |
|                     | 2                    | 0.782                                       | 0.876  | 12.02  |
|                     | 1                    | 0.830                                       | 0.929  | 11.92  |
| Clay + silt + sand  | $\infty$             | 0.784                                       | 0.878  | 11.98  |
|                     | 2                    | 0.801                                       | 0.897  | 11.98  |
|                     | 1                    | 0.828                                       | 0.927  | 11.95  |
| Silt + sand         | $\infty$             | 0.749                                       | 0.838  | 11.88  |
|                     | 2                    | 0.786                                       | 0.880  | 11.95  |
|                     | 1                    | 0.822                                       | 0.920  | 11.92  |

**FIGURE 6**  $(I(\text{with harmonics})/I(90))$  versus the thermal resistivity of the backfill soil.

underground cables using the FEM in the case of steady-state thermal equilibrium, Equation (27) can be used<sup>19</sup>

$$\frac{\partial}{\partial x} \left[ \frac{1}{\rho} \frac{\partial \theta}{\partial x} \right] + \frac{\partial}{\partial y} \left[ \frac{1}{\rho} \frac{\partial \theta}{\partial y} \right] + q = 0, \quad (27)$$

where  $\theta$  is defined as the temperature of point  $(x, y)$ ,  $\rho$  denotes the thermal resistivity of the medium in K m/W,

**FIGURE 7** Impact of the cable laying depth on the ratio between the cable conductor temperature in the presence of harmonics and the maximum permissible conductor temperature of the cable for an 11 kV cable.

and  $q$  represents the heat generated by the cable losses per unit volume in  $\text{W/m}^3$ . In any homogeneous area of a specified thermal resistivity and heat generation rate, the temperature at point  $(x, y)$  in the region subjected to

specified boundary conditions can be obtained by solving Equation (27). The power cable and its surrounding backfill material can be divided into very small triangles, forming a mesh as illustrated in Figure 8. Adiabatic boundaries are set on both left and right sides far away from the cable and the top and the bottom of the installation (i.e., heat flux equals zero). The interface boundary between the soil and the air is considered a thin layer boundary, which is used to define the thermal resistivity and thermodynamic properties of this interface. The soil surface is simulated as an isothermal boundary at air temperature. This set of boundary conditions results in a negligible mistake in temperature calculations. The maps of the temperature distribution of the cable elements and its backfill soil are carried out using the FEM and COMSOL multiphysics program.<sup>40,41</sup>

The influence of the external environmental condition is simulated by the variation in air temperature surrounding the cable route, which in turn is reflected in the temperature's distribution of the cable components and the cable backfill soil, as shown in Figure 9 at 30°C and 40°C air temperatures.

Figures 10 and 11 illustrate the temperature distribution of the cable components and the backfill soil only, without the part of the air that surrounds the cable route,

with and without the impact of harmonics. The cable current is 2.04 kA per phase, and the cable is buried at a laying depth equal to 1.5 m in the sandy soil; the thermal resistivity of the backfill soil was 1.2 K m/W in Figure 10 and equal to 2 K m/W in Figure 11, respectively. The ambient temperature is 35°C. Comparing Figures (A) and (B) of Figures 9, 10, and 11, it is observed that a significant increase in the cable core temperature is carried out in the harmonic occurrence compared to its absence. Finally, it is observed that the obtained results are in good agreement with both the measured results and analytical results that are given by the proposed analytical method. The external dimensions of the computational domains of Figures 9, 10, and 11 are (10 m × 8 m), more sizes gave similar results. The dimensions shown in these figures are zoomed in the figures to show the temperature of the cable and surrounding soils accurately.

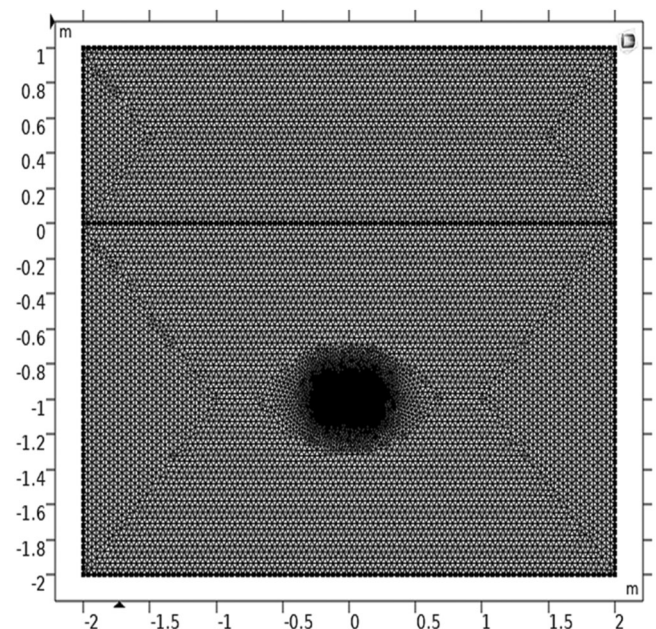


FIGURE 8 Finite element method modeling.

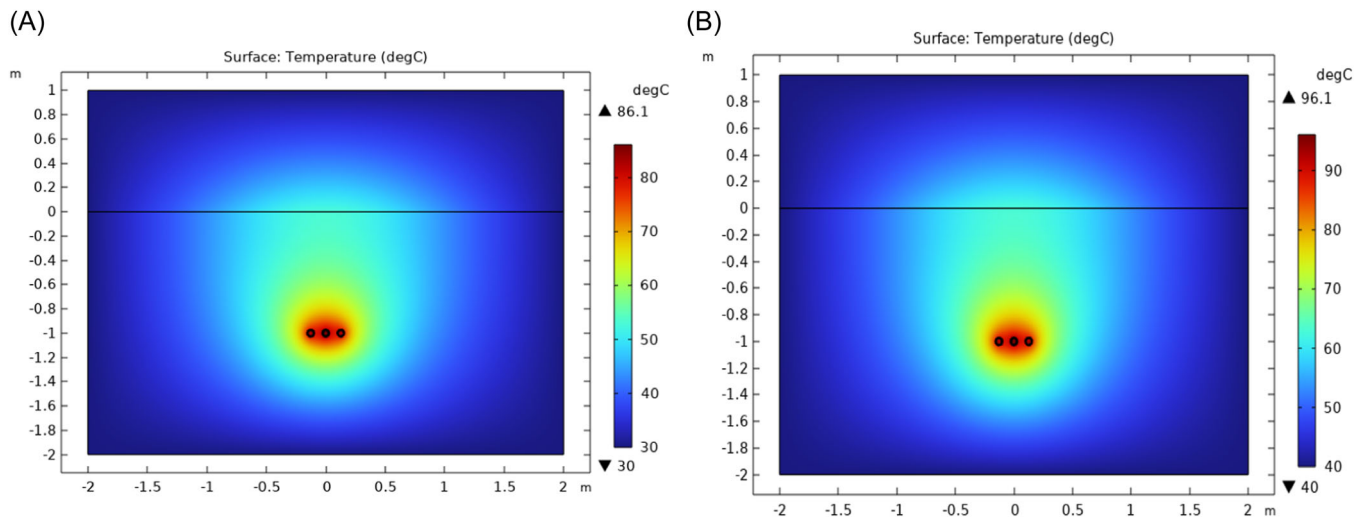
TABLE 6 Impact of the cable laying depth on the cable conductor temperature in the presence of harmonics.

| Cable laying depth  | $D = 0.5 \text{ m}$ | $D = 1 \text{ m}$ | $D = 1.5 \text{ m}$ |
|---|---------------------|-------------------|---------------------|
| $\theta_{H,A,\text{temperature}} (^{\circ}\text{C})$      | 94.001              | 104.151           | 110.087             |
| $\theta_{H,B,\text{temperature}} (^{\circ}\text{C})$      | 94.012              | 106.076           | 110.123             |
| $\theta_{H,C,\text{temperature}} (^{\circ}\text{C})$      | 94.001              | 104.151           | 110.087             |
| $\theta_{H,\text{sheath,temperature}} (^{\circ}\text{C})$ |                     |                   |                     |
| A   | 74.537              | 82.585            | 87.346              |
| B   | 77.667              | 87.633            | 90.976              |
| C   | 74.537              | 82.585            | 87.346              |

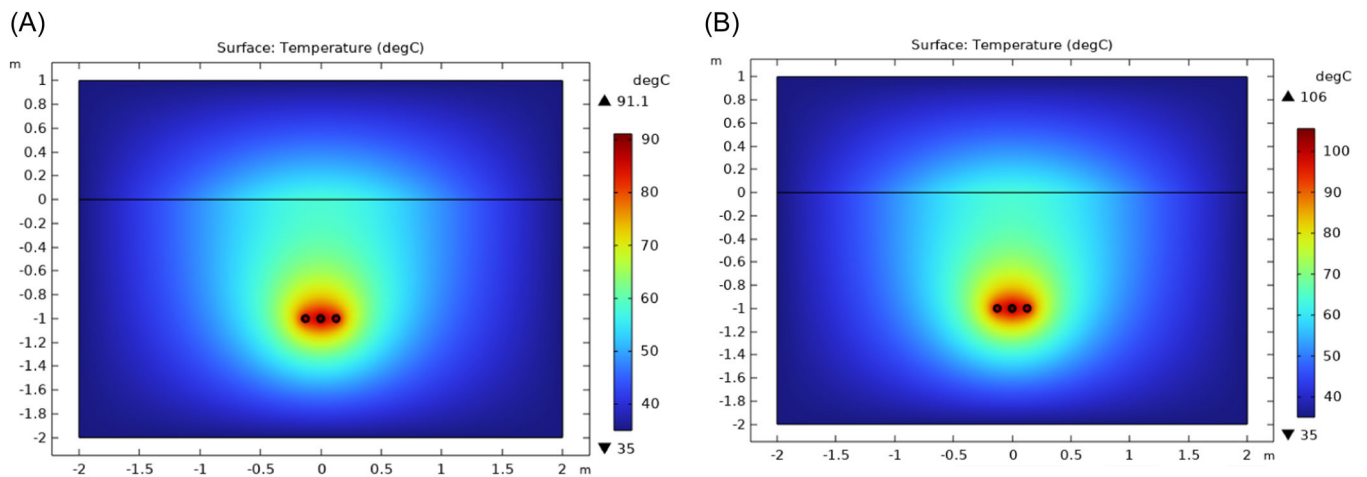
| Cable phase   | $s = 127 \text{ mm}$ | $s = 150 \text{ mm}$ | $s = 175 \text{ mm}$ | $s = 200 \text{ mm}$ |
|---|----------------------|----------------------|----------------------|----------------------|
| $\theta_{H,A} (^{\circ}\text{C})$                         | 104.151              | 104.091              | 104.027              | 103.963              |
| $\theta_{H,B} (^{\circ}\text{C})$                         | 106.076              | 106.001              | 105.938              | 105.867              |
| $\theta_{H,C} (^{\circ}\text{C})$                         | 104.151              | 104.091              | 104.027              | 103.963              |
| $\theta_{H,\text{sheath,temperature}} (^{\circ}\text{C})$ |                      |                      |                      |                      |
| A   | 82.585               | 82.537               | 82.487               | 82.436               |
| B   | 87.633               | 87.571               | 87.519               | 87.46                |
| C   | 82.585               | 82.537               | 82.487               | 82.436               |

TABLE 7 Effect of the axial spacing between cables on the core cable temperature.





**FIGURE 9** Temperature distribution of the cable components and the backfill soil with the impact of harmonics on sandy soil ( $\rho_{\text{soil}} = 1.2 \text{ K m/W}$ ): (A) air temperature 30°C and (B) air temperature 40°C.



**FIGURE 10** Temperatures distribution of the cable components and the backfill soil with and without the impact of harmonics on wet sandy soil ( $\rho_{\text{soil}} = 1.2 \text{ K m/W}$ ): (A) without and (B) with the influence of harmonics.

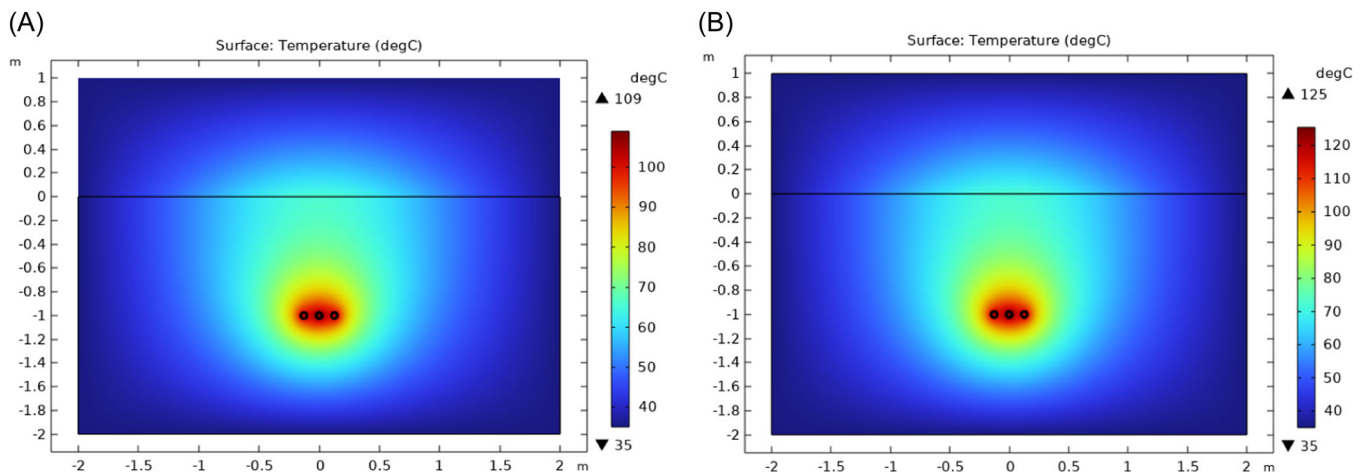


**FIGURE 11** Temperature distribution of the cable components and the backfill soil with and without the impact of harmonics on dry sandy soil ( $\rho_{\text{soil}} = 2 \text{ K m/W}$ ): (A) without and (B) with the influence of harmonics.



## 6 | CONCLUSIONS

This article is characterized by a study of the thermal effect of harmonics on cable loaded by nonlinear loads for medium-voltage cables. The effect of the soil components surrounding the cable was taken into account during the year's seasons. The calculated results are confirmed by site measurements. In this paper, the proposed algorithm based on the heat equilibrium of the nodes of the thermal circuit of a medium-voltage cable system is used to investigate the impact of harmonics on the performance of the medium-voltage underground cables in flat formation.

From the obtained results, it is concluded that the impact of harmonics on the underground power cable temperature have been considered to re-evaluate the cable capacity and avoid the thermal failure of the cable insulation.

It is noticed that the combination of the presence of harmonics in the cable core with the formation of a dry zone around the cable increases the cable core temperature to severe values and has a significant influence on the cable current, especially when it is buried in the soil of a high thermal resistivity at summer season ( $pf = \infty$ ). The core temperature reached in summer ( $pf = \infty$ ) to 152.162°C, 139.053°C, and 133.375°C when lime, sand, and silt + sand are used as backfill materials, respectively, rather than 90°C. It is observed also that with the increase of the soil thermal resistivity, the ratio of ( $\theta_H / \theta_{\text{without harmonics}}$ ) reaches about 1.2 times when soil thermal resistivity equals 2.5 K m/W.


In addition, it is noticed that the percentage reduction of the derating factor of the center cable caused by the impact of harmonics differs between 11.88% and 12.37% depending on the backfill soil composition. Using the proposed algorithm can save laboratory measurements, which usually require a long time and costly preparations. This algorithm can also be used in the investigation of the impact harmonics on cables in trefoil formation.

## ACKNOWLEDGMENTS

The authors acknowledge the support grant received from the Department of Electrical Engineering and Automation, School of Electrical Engineering, Aalto University, Espoo, Finland.

## ORCID

Adel Z. El Dein  <https://orcid.org/0000-0001-9614-1753>

Elsayed Tag-Eldin  <https://orcid.org/0000-0003-3151-9967>

Matti Lehtonen  <https://orcid.org/0000-0002-9979-7333>

Mohamed M. F. Darwish  <https://orcid.org/0000-0001-9782-8813>

## REFERENCES

1. Hiranandani AK. Effects of harmonics on the current carrying capacity of insulated power cables used in three phase electrical power distribution systems. In: *CIREC 2005—18th International Conference and Exhibition on Electricity Distribution*, Turin, Italy, IEEE; 2005:1-5.
2. Sahin YG, Aras F. Investigation of harmonic effects on underground power cables. In: *2007 IEEE International Conference on Power Engineering, Energy and Electrical Drives (POWERENG)*, April 12-14, 2007, Setubal, Portugal, IEEE; 2007:589-594.
3. O'Connell K, Barrett M, Blackledge J, Sung A. Cable heating effects due to harmonic distortion in electrical installations. In: *Proceedings of the World Congress on Engineering 2012 (WCE 2012)*, London, UK, International Association of Engineers: ICEEE12; Vol. II, 2012:1-6.
4. Subjak JS, McQuilkin JS. Harmonics—causes, effects, measurements, and analysis: an update. *IEEE Trans Ind Appl*. 1990;26(6):1034-1042.
5. Wagner VE, Balda JC, Griffith DC, et al. Effects of harmonics on equipment, report of the IEEE task force on the effects of harmonics on equipment. *IEEE Trans Power Del*. 1993;8(2):672-680.
6. Carpinelli G, Caramia P, Di Vito E, Losi A, Verde P. Probabilistic evaluation of the economic damage due to harmonic losses in industrial energy system. *IEEE Trans Power Del*. 1996;11(2):1021-1028.
7. Emanuel AE, Yang M. On the harmonic compensation in non-sinusoidal systems. *IEEE Trans Power Deliv*. 1993;8(1):393-399.
8. Desmet JJM, Sweertvaegher I, Vanalme G, Stockman K, Belmans R. Analysis of the neutral conductor current in a three-phase supplied network with nonlinear single-phase loads. *IEEE Trans Ind Appl*. 2003;39(3):587-593.
9. Shafiee Rad M, Kazerooni M, Jawad Ghorbany M, Mokhtari H. Analysis of the grid harmonics and their impacts on distribution transformers. In: *IEEE Power and Energy Conference at Illinois (PECI)*, Champaign, IL, USA, IEEE; 2012:1-5.
10. Rice DE. Adjustable speed drive and power rectifier harmonics their effect on power system components. *IEEE Trans Ind Appl*. 1986;IA-22(1):161-177.
11. International Electrotechnical Commission. IEC60 287-1-1 "Electric Cables—Calculation of the Current Rating—Part 1-2". IEC; 1994.
12. Electrical Installations of Buildings—Part 5: Selection and Erection of Electrical Equipment—Section 523: Current-Carrying Capacities in Wiring Systems, CENELEC Std., HD384.5.523, S2:2001. Accessed October 15, 2022. <https://standards.iteh.ai/catalog/standards/clc/0960b751-fcb1-4215-85ef-018bdda7289c/hd-384.5.523-s2-2001>
13. International Electrotechnical Commission. IEC60364: 2002-06—*Electrical Installations of Buildings*. 2nd ed. IEC; 2002.
14. Electro-Technical Council of Ireland. ET101: *National Rules for Electrical Installations*. 4th ed. ETCI; 2004.
15. Electrical and Mechanical Services Department. *Code of Practice for the Electricity (Wiring) Regulations*. 1997 ed. EMSD; 1997.
16. The Institute of Engineering and Technology. *BS 7671—18th Edition, The IET Wiring Regulations Information and Help for Electrical Installers*. IET; 2019.

17. Sakis Meliopoulos AP, Martin Jr. MA Calculation of secondary cable losses and ampacity in the presence of harmonics. *IEEE Trans Power Del.* 1992;7(2):451-457.
18. Neher JH, McGrath MH. The calculation of the temperature rise and load capability of cable systems. *AIEE Trans.* 1957;76: 752-772.
19. Nahman J, Tanaskovic M. Determination of the current carrying capacity of cables using the finite element method. *Electr Power Syst Res.* 2002;61:109-117.
20. Institute of Electrical and Electronics Engineers. *IEEE Recommended Practices and Requirements for Harmonic Control in Electrical Power Systems*, IEEE Std. 519-1992. IEEE; 1993.
21. International Electrotechnical Commission. *IEC 61000-3-2:2018. Electromagnetic Compatibility (EMC)—Part 3-2: Limits for Harmonic Current Emissions (Equipment Input Current ≤16 A Per Phase)*. IEC; 2018.
22. Sivaraman P, Sharmela C. Power system harmonics. In: Sanjeevikumar P, Sharmela C, Holm-Nielsen JB, Sivaraman P, eds. *Power Quality in Modern Power Systems*. Academic Press; 2021:61-103.
23. Alkahtani AA, Alfalahi S, Athamneh AA, et al. Power quality in micro-grids including supra-harmonics: issues, standards, and mitigations. *IEEE Access.* 2020;8:127104-127122.
24. Senthil Kumar R, Surya Prakash R, Yokesh Kiran B, Sahana A. Reduction and elimination of harmonics using power active harmonic filter. *Int J Recent Technol Eng.* 2019;8: 178-184.
25. Park B, Lee J, Yoo H, Jang G. Harmonic mitigation using passive harmonic filters: case study in a steel mill power system. *Energies.* 2021;14:2278.
26. Lumberras D, Gálvez E, Collado A, Zaragoza J. Trends in power quality, harmonic mitigation and standards for light and heavy industries: a review. *Energies.* 2020;13:5792.
27. Nazirov KB, Ganiev ZS, Dzhuraev SD, Ismoilov ST, Rahimov RA. Elaboration of the method for providing the level of power quality in the nodes of the energy system while power quality monitoring. In: *Proceedings of the 2020 IEEE Conference of Russian Young Researchers in Electrical and Electronic Engineering, EIconRus 2020, St. Petersburg and Moscow, Russia, January 27-30, 2020*. IEEE; 2020:1282-1286.
28. Ahir J, Upadhyay C. Harmonic analysis and mitigation for modern home appliances. In: *Proceedings of the 4th International Conference on Electrical Energy Systems, ICEES 2018, Chennai, India, Institute of Electrical and Electronics Engineers Inc.*; 2018:218-223.
29. Messtechnik E. *EN 50160 Report—Power Quality Standard*. NEO Messtechnik; 2021. Accessed December 15, 2022. <https://www.neo-messtechnik.com/en/power-quality-explained-chapter5-en-50160-report-standard>
30. Gouda OE, Dein AZE. Enhancement of the thermal analysis of harmonics impacts on low voltage underground power cables capacity. *Electr Power Syst Res.* 2022;204: 107719.
31. Shazly JH, Mostafa MA, Ibrahim DK, Abo El Zahab EE. Thermal analysis of high-voltage cables with several types of insulation for different configurations in the presence of harmonics. *IET Gener Transm Distrib.* 2017;11(14):3439-3448.
32. Hiranandani A. Calculation of cable ampacities including the effects of harmonics. *IEEE Ind Appl Mag.* 1998;4(2):42-51.
33. Demoulias C, Labridis DP, Dokopoulos PS, Gouramanis K. Ampacity of low-voltage power cables under non-sinusoidal currents. *IEEE Trans Power Deliv.* 2007;22(1):584-594.
34. Yong J, Xu W. A method to estimate the impact of harmonic and unbalanced currents on the ampacity of concentric neutral cable. *IEEE Trans Power Deliv.* 2016;31(5):1971-1979.
35. Demoulias C. Ampacity of low-voltage power cables under non-sinusoidal currents. *IEEE Trans Power Appar Syst.* 2007;22(1): 584-593.
36. International Electrotechnical Commission. *IEC Standard 61000-4-7: "Electromagnetic Compatibility (EMC)—Part 4-7: Testing and Measurement Techniques—General Guide on Harmonics and Inter-Harmonics Measurements and Instrumentation, For Power Supply Systems and Equipment Connected Thereto"*. IEC; 2008.
37. Gouda O, Abdelaziz A, Refaie R, Matter Z. Experimental study for drying-out of soil around underground power cables. *J King Abdulaziz Univ Eng Sci.* 1997;9:23-40.
38. Gouda OE, Amer GM, El Dein AZ. Improving the underground cables ampacity by using artificial backfill materials. In: *Proceedings of the 14th International Middle East Power Systems Conference (MEPCON'10), December 19-21, 2010, Cairo University, Egypt*, IEEE; 2010:38-43.
39. Gouda OE, Amer GM, El Dein AZ. Effect of the formation of the dry zone around underground power cables on their ratings. *IEEE Trans Power Deliv.* 2010;26(2):972-978.
40. Kellow M. A numerical procedure for the calculation of the temperature rise and ampacity of underground cables. *IEEE Trans Power Appar Syst.* 1981;PAS-100:3322-3330.
41. Hwang CC, Jiang YH. Extensions to the finite element method for thermal analysis of underground cable systems. *Electr Power Syst Res.* 2003;64(2):159-164.

**How to cite this article:** Gouda OE, El Dein AZ, Tag-Eldin E, Lehtonen M, Darwish MMF. Thermal analysis of the influence of harmonics on the current capacity of medium-voltage underground power cables. *Energy Sci Eng.* 2023;1-15. doi:10.1002/ese3.1534